COMPETITIVE CHEMICAL REACTIONS IN DC POLAROGRAPHY: INFLUENCE OF FAST PROTONATION EQUILIBRIA ON CE AND ECE MECHANISMS

Eulogia MUÑOZ, José L. AVILA, Juan J. RUIZ and Luis CAMACHO*

Department of Physical Chemistry and Applied Thermodynamics, Faculty of Sciences, University of Córdoba, 14004 Córdoba, Spain

Received April 23, 1990
Accepted June 22, 1990

Dedicated to the memory of Prof. J. Heyrovský on the occasion of his centenary.

We carried out a DC polarographic study of the limiting current for CE and ECE processes with chemical stages subject to potential catalytic effects and in direct competition with protonation reactions in quasi-equilibrium. The aforesaid competition may result in the appearance of maxima in the limiting current vs pH plots for CE mechanisms. We established the conditions required for the rise of such maxima, and developed methods for the calculation of kinetic parameters. The competition did not result in any maxima in the above-mentioned plots for ECE mechanisms; however, we established criteria for their potential identification.

Dehydration and deamination reactions usually yield kinetic waves in DC polarography. Such is the case with the reduction of carbonyl compounds and hydroxylamines. In both cases, like in other similar instances, the reduction mechanisms involved are commonly affected by protonation equilibria, which are generally faster than the aforesaid reactions.

Thus, a number of carbonyl compounds undergo processes of the CE type in basic media according to Scheme 1.

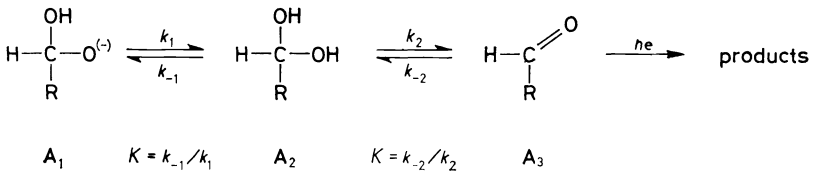

SCHEME 1

* All correspondence concerning this paper should be addressed to: Dr Luis Camacho, Departamento de Química Física y Termodinámica Aplicada, Facultad de Ciencias, Universidad de Córdoba, 14004 Córdoba, Spain.

The second equilibrium is often shifted to the hydrated form, i.e. $K_2 \gg 1$. This reaction scheme can account for the occurrence of maxima in the plots of the limiting current (i_L) as a function of pH, as reported by a number of authors[1-7].

Another typical example is the reduction of amides, which undergo ECE processes[8-10]. The kinetic character of the waves they yield arises from the slow deamination of the hydroxyamine intermediate. In acid media, the reduction of these compounds takes places according to Scheme 2 (refs[8-10]).

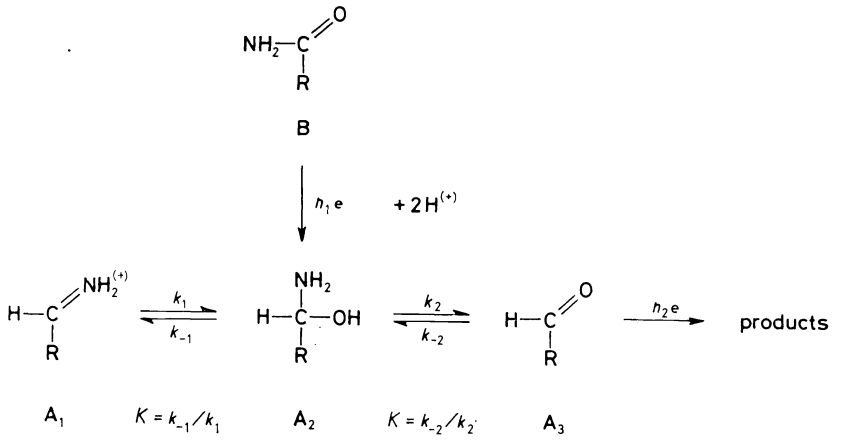

SCHEME 2

Only a single wave is obtained by DC polarography; it results from the joint reduction of species B and A_3. Species A_1 is also electroactive, though its reduction potential is much more negative than that of the previous species, so its reduction at a very acid pH is masked by the discharge of the supporting electrolyte[10].

In Scheme 2, the deamination reaction is usually markedly shifted to the keto form, i.e. $K_2 \ll 1$.

As stated above, and for the two schemes, the protonation equilibrium is rather fast, i.e. $(k_1 + k_{-1}) \gg (k_2 + k_{-2})$.

The reduction of *p*-nitrophenol[11] and *o*-nitrophenol[12] also takes place through a mechanism similar to that represented by Scheme 2. Thus, in the first step, these compounds are reduced by exchanging 4 electrons per molecule, yielding the hydroxyphenylhydroxyamine derivative which, at a basic pH, undergoes competitive dissociation of an H^+ ion, which in turn gives rise to an electroinactive anion or a slow dehydration process to the electroactive imine; this, finally, is reduced by exchanging two electrons per molecule.

The equations representing Schemes 1 and 2 were derived by ourselves in their general form earlier[7,11]. Their complexity, however, hinders a simple study of the properties of their solutions.

Nevertheless, if the above-mentioned conditions (i.e., $K_2 \gg 1$ for CE and $K_2 \ll 1$ for ECE mechanisms) are taken into account, the solutions become much simpler and straightforward expressions allowing the analytical determination of the corresponding kinetic parameters can be established. Obtaining such approximations and developing appropriate methods of analysis are the chief aims of this work.

We should note that the two mechanisms studied here (Schemes 1 and 2) are kinetically indistinguishable from those where the protonation equilibrium is established directly between species A_1 and A_3 rather than between A_1 and A_2. This extends the applicability of the expressions below to a wider range of examples.

THEORETICAL

CE *Mechanism*

With slight modifications in the terminology, the equation for the limiting current in Scheme 1 was[7]:

$$\frac{I}{1-I} = \frac{F(\lambda_1)\,F(\lambda_2)\{r_{21} - r_{11}\}}{F(\lambda_2)\,r_{13}\{1 - r_{21}\} - F(\lambda_1)\,r_{23}\{1 - r_{11}\}}, \tag{1}$$

where

$$I = i_L/i_D \tag{2}$$

$$\lambda_1 = \tfrac{1}{2}k\,(1 + \gamma), \quad \lambda_2 = \tfrac{1}{2}k\,(1 - \gamma) \tag{3), (4}$$

$$k = k_1(1 + K_1) + k_2(1 + K_2) \tag{5}$$

$$\gamma = \left(1 - \frac{4s}{k^2}\right)^{1/2} \tag{6}$$

$$s = k_1 k_2 K \tag{7}$$

$$K = 1 + K_2 + K_1 K_2 \tag{8}$$

$$r_{i1} = \frac{k_1}{k_1 - \lambda_i}, \quad r_{i3} = \frac{k_{-2}}{k_{-2} - \lambda_i}, \quad \text{for} \quad i = 1, 2 \tag{9), (10}$$

$$F(\lambda_i) = (1{\cdot}349\,\sqrt{(t\lambda_i)}])^{1{\cdot}091}\coth(1{\cdot}349\,\sqrt{(t\lambda_i)}])^{1{\cdot}091}, \tag{11}$$

where t is the drop time and i_D is the diffusion current. Equation (*1*) can be modified by substituting the r_{ij} terms, which, after some further transformations, yields:

$$\frac{I}{1-I} = \frac{F(\lambda_1)\,F(\lambda_2)\,k_1(k_1 - k_{-2})\,(\lambda_1 - \lambda_2)}{K_2\{F(\lambda_2)\,\lambda_2(\lambda_2 - k_{-2})\,(\lambda_1 - k_1) - F(\lambda_1)\,\lambda_1(\lambda_1 - k_{-2})\,(\lambda_2 - k_1)\}}. \tag{12}$$

If, as stated in the introduction, we assume $K_2 \gg 1$ and $k_2 \to 0$, then Eq.(6) can be rewritten as:

$$\gamma = \frac{\{k_1(1 + K_1) - k_{-2}\}}{\{k_1(1 + K_1) + k_{-2}\}} . \qquad (13)$$

which, substituted into Eqs (3) and (4), yields:

$$\lambda_1 = k_1(1 + K_1) , \quad \lambda_2 = k_{-2} . \qquad (14), (15)$$

Thus, Eq. (12) can be simplified to:

$$\frac{I}{1 - I} = \frac{\mathrm{F}(\lambda_2)}{K_2(1 + K_1)} . \qquad (16)$$

If $(\lambda_2 t) > 10$, which seems quite logical for most of the examples considered, Eq. (11) can be approximated to:

$$\mathrm{F}(\lambda_i) \cong 1{\cdot}349\ (\lambda_i t)^{1/2} . \qquad (17)$$

According to Scheme 1, and for buffered media, K_1 will be an apparent equilibrium constant such that $K_1 = k_1^0/[\mathrm{H}^+]$. Likewise, the dehydration reaction is usually subject to acid-base catalysis[7,13-15]. If only base catalysis is considered, then:

$$k_{-2} = k_2^0 + k_2^{\mathrm{OH}}[\mathrm{OH}^-] . \qquad (18)$$

Thus, Eq. (16) can be rewritten as:

$$\frac{I}{1 - I} = 1{\cdot}349 \left(\frac{k_2^0 t}{K_2}\right)^{1/2} \frac{\left(1 + \frac{k_2^{\mathrm{OH}} K_{\mathrm{W}}}{k_0^2}\, 10^{\mathrm{pH}}\right)}{(1 + K_1^0\, 10^{\mathrm{pH}})} . \qquad (19)$$

The analysis of this equation allows one to predict that the plot of I vs pH will show a maximum provided

$$k_2^{\mathrm{OH}} K_{\mathrm{W}}/k_2^0 > 2K_1^0 . \qquad (20)$$

Accordingly, at $\mathrm{pH} \ll -\log(k_2^{\mathrm{OH}} K_{\mathrm{W}}/k_2^0)$ (neutral and acid pH values in the example illustrated in Fig. 1 in the following section), I will be constant as the pH-dependent terms in Eq. (19) are much smaller than unity. This allows the k_2^0/K_2 ratio to be readily calculated. Under this assumption, Eq. (19) coincides with that of a simple kinetic CE process[16,17]. The constant value 1·349 in this equation is not the same as that ion the Koutecký equation[16] as this author used mean currents.

Our solution is closer to the approximations reported by other authors who, like us, used maximal currents[17]. I increases with the pH, provided the condition expressed by Eq. (*20*) is met, and reaches a maximum at the pH value given by

$$(\mathrm{pH})_M = \mathrm{p}K_1 + \log\left(1 - \frac{2K_1^0 k_2^0}{k_2^{OH} K_W}\right). \tag{21}$$

The maximum current at the pH given in Eq. (*21*), I_M will be given by

$$\frac{I_M}{1 - I_M} = 1{\cdot}349\left(\frac{k_2^0 t}{K_2}\right)^{1/2} \frac{\left(\frac{k_2^{OH} K_W}{K_1^0 k_2^0} - 1\right)^{1/2}}{2\left(1 - \frac{K_1 k_2^0}{k_2^{OH} K_W}\right)}. \tag{22}$$

Finally, I decreases with increasing pH above the value given by Eq. (*21*). This behaviour is rather common in carbonyl compounds in basic media.

The non-fulfillment of Eq. (*20*) leads to an I–pH plot with no maxima, i.e. I decreases monotonously with the pH.

ECE *Mechanism*

According to the solution reported in the literature[10], the limiting current for Scheme 2 is given by:

$$I = \frac{n_1 + n_2\varphi}{n_1 + n_2} = \frac{i_L}{i_D^T} \tag{23}$$

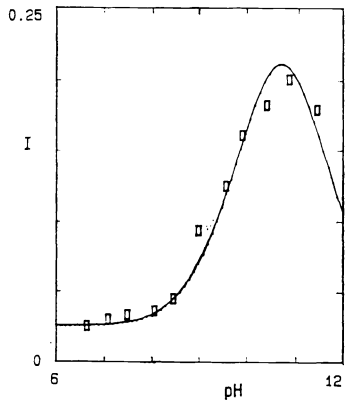

FIG. 1

Plot of $I = i_L/i_D$ vs pH. The boxes correspond to the experimental results for the second reduction wave of glyoxal at neutral and basic pH values, with $C = 1{\cdot}25 \,.\, 10^{-2}$ mol dm^{-3} and $i_D = 100\,\mu$A. The solid line corresponds to the application of Eq. (*19*), where $K_1^0 = 1{\cdot}78 \,.\, 10^{-11}$, $k_2^0/K_2 = 8{\cdot}958 \,.\, 10^{-5}$, $k_2^{OH}K_W/k_2^0 = 7{\cdot}7 \,.\, 10^{-9}$ and $t = 4$ s

with

$$\varphi = \frac{F(\lambda_2)(r_{21} - 1)(F(\lambda_1) - 1) - F(\lambda_1)(r_{11} - 1)(F(\lambda_2) - 1)}{F(\lambda_2)(F(\lambda_1) - r_{13})(r_{21} - 1) - F(\lambda_1)(F(\lambda_2) - r_{23})(r_{11} - 1)}, \quad (24)$$

where Eqs (3)–(11) are still valid and i_D^T is the diffusion current corresponding to the exchange of $n_1 + n_2$ electrons. For simplicity in the analysis, it is more convenient to use the $(1 - \varphi)/\varphi$ function. By removing the r_{ij} terms from such a function, one has:

$$\frac{1 - \varphi}{\varphi} = \frac{K(k_1(\lambda_1 F(\lambda_1) - \lambda_2 F(\lambda_2)) - k_1(F(\lambda_1) - F(\lambda_2))(k_2 K + k_{-2}) + k_{-2}(\lambda_2 F(\lambda_1) - \lambda_1 F(\lambda_2)))}{(k_1 - k_{-2})(F(\lambda_1) F(\lambda_2)(\lambda_1 - \lambda_2) + k_2 K(F(\lambda_1) - F(\lambda_2)) - \lambda_1 F(\lambda_1) + \lambda_2 F(\lambda_2))}. \quad (25)$$

Let us assume, as stated in the introduction, that $K_2 \gg 1$ and $k_{-2} \to 0$. Let us also assume that the protonation equilibrium is very fast, i.e. k_1 and $k_{-1} \gg k_2$. Under these conditions:

$$\lambda_1 = k_1(1 + K_1), \quad (26)$$

$$\lambda_2 = k_2/(1 + K_1). \quad (27)$$

By substituting these into Eq. (25), one has:

$$\frac{1 - \varphi}{\varphi} = \frac{1}{F(\lambda_2) - 1}. \quad (28)$$

Provided $\lambda_i t \leqq 0{\cdot}15$, and with an error less than 5%, we may write:

$$F(\lambda_1) \cong 1 + 0{\cdot}91 t\lambda_i. \quad (29)$$

Because of the range of $\lambda_i t$ values over which ECE mechanisms yield kinetic waves in DC polarography, neither Eq. (17) nor Eq. (29) can be applied; however, they can be used to analyse the behaviour trends at small and large values of the kinetic parameters.

By denoting the diffusion corresponding to the exchange of n_1 electrons by i_D^1, one has:

$$\frac{i_D^T - i_L}{i_L - i_D^1} = \frac{1 - \varphi}{\varphi}. \quad (30)$$

Likewise, if, as above, the medium is assumed to be buffered, i.e. $K_1 = K_1^0[H^+]$, then λ_2 will range between k_2/K_1 at pH $\ll$ pK_1 and k_2 at pH $\gg$ pK_1. In the latter case, i_L and φ will reach maximum values we shall denote by i_M and φ_M, respectively (see Fig. 2 in the following section); thus:

$$\frac{i_D^T - i_M}{i_M - i_D^1} = \frac{1 - \varphi_M}{\varphi_M} = \frac{1}{F(k_2) - 1}, \tag{31}$$

i_L and φ will decrease with decreasing pH, so $\varphi \to 0$ and $i_L \to i_D^1$.

Let us define

$$\frac{i_M - i_L}{i_L - i_D^1} = \frac{\varphi_M - \varphi}{\varphi} = \frac{F(k_2) - F(\lambda_2)}{F(k_2)\{F(\lambda_2) - 1\}}. \tag{32}$$

As long as k_2 is small enough, Eq. (*29*) will be applicable throughout the pH range, in which case:

$$\frac{i_M - i_L}{i_L - i_D^1} = \frac{K_1^0[H^+]}{1 + 0{\cdot}91k_2t} \tag{33}$$

which, in logarithmic form, reveals a linear pH-dependence of slope -1.

If k_2 is large enough for Eq. (*17*) to be accurate, then Eq. (*33*) will still be valid if $i_L \to i_D^1$. However, if $i_L \to i_D^T$, Eq. (*17*) can be applied to $F(\lambda_2)$ in Eq. (*32*) in which case:

$$\frac{i_M - i_L}{i_L - i_D^1} = \frac{K_1^0[H^+]}{2{\cdot}698(k_2t)^{1/2}}. \tag{34}$$

The logarithmic form of this equation shows the same pH-dependence as Eq. (*33*), although the intercept is somewhat different.

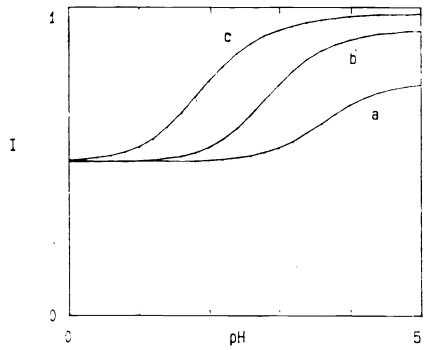

FIG. 2

Plot of I vs pH. The I values were obtained from Eq. (*32*) by assuming $n_1 = n_2$, $K_1^0 = 10^4$, $t = 4$ s, and (curve a) $k_2 = 0{\cdot}5$ s, (curve b) $k_2 = 5$ s and (curve c) $k_2 = 50$ s

Note that the effect of acid catalysis on k_2 can never lead to the occurrence of maxima in the i_L–pH plots for this type of mechanism. The potential influence of catalysis on k_2 will be discussed in the following section.

ANALYTICAL CRITERIA

CE *Mechanism*

The simplicity of Eqs (*19*) and (*32*) allows the ready analysis of the experimental results. Thus, for the CE mechanism, the plot of $\log [I/(1 - I)]$ vs pH should be linear, with a slope of $-0{\cdot}5$ at pH $< (\mathrm{pH})_M$ (see Eqs (*19*) and (*21*)). At pH $> (\mathrm{pH})_M$, the aforesaid plot should again be linear, but with a slope of $+0{\cdot}5$. A prior knowledge of i_D and K_2 should allow the problem to be fully solved.

A more accurate working procedure involves using Eqs (*21*) and (*22*). In fact, as stated above, the k_2^0/K_2 ratio can be calculated from the pH region where I is constant. Once I_M is known, Eq. (*22*) allows the $k_2^{OH}K_W/k_2^0K_1^0$ ratio to be calculated, and once $(\mathrm{pH})_M$ is known (Eq. (*21*)), we can evaluate K_1^0 and $k_2^{OH}K_W/k_2^0$ individually. These results can be used as the starting point for a more accurate numerical fitting of the experimental results.

Figure 1 shows the plot of I vs pH obtained from Eq. (*19*) by using the following values: $K_1^0 = 1{\cdot}78 \,.\, 10^{-11}$, $k_2^0/K_2 = 8{\cdot}958 \,.\, 10^{-5}$, $k_2^{OH}K_W/k_2^0 = 7{\cdot}7 \,.\, 10^{-9}$ and $t = 4$s.

The figure also shows the experimental variation of I with the pH for the second reduction wave of glyoxal at a basic pH (boxes). These experimental data were reproduced from ref.[4], where the glyoxal concentration used was $1{\cdot}25 \,.\, 10^{-2}$ mol dm^{-3}. Likewise, i_D was estimated to be 100 μA – the value used in our calculations – at such a concentration.

ECE *Mechanism*

The most accurate criterion for the analysis of Scheme 2 involves the numerical fitting of the experimental i_L–pH curves by using Eq. (*32*). However, in the absence of catalysis, it is simpler to use a logarithmic plot as a function of the pH such as that predicted by Eqs (*33*) and (*34*).

Figure 2 shows the plot of I vs pH for three examples, with $n_1 = n_2$, $K_1^0 = 1 \,.\, 10^4$, $t = 4$ s, and curve (a) $k_2 = 0{\cdot}5$ s, curve (b) $k_2 = 5$ s and curve (c) $k_2 = 50$ s.

Figure 3 shows the plot of $\log [(i_M - i_L)/(i_L - i_D^1)]$ vs pH for all three cases in the previous figure. For cases (a) and (b), the plot is linear, with a slope of -1, consistent with the prediction of Eq. (*33*).

In view of these results, the applicability range of Eq. (*33*) is much wider than that resulting from the strict fulfillment of Eq. (*28*). In case (curve c) in Fig. 3, the aforesaid plot is linear, with a slope of -1 for $\log [(i_M - i_L)/(i_L - i_D^1)]$ values between $+2$

and $-0{\cdot}4$, i.e. the range over which Eq. (*33*) is applicable. At values below -1, the plot in Fig. 3 is again linear, with a slope of -1 according to Eq. (*34*). There are deviations from linearity in the intermediate region. The application of Eq. (*34*) to the example considered is experimentally unfeasible as it is only useful for i_L values differing by less than 10% from the i_M value.

The influence of acid catalysis on k_2 is reflected in Fig. 4, where all parameters have the same values as in the previous case, with the exception of $K_1^0 = 10^3$ and k_2, which was assumed to be $k_2 = k_2^0 + k_2^H[H^+]$, with $k_2^0 = 0{\cdot}5$ and $k_2^H = 0$ (curve a), 10^3 (curve b) and 10^5 s^{-1} (curve c).

As can be seen, the limiting current of the process is a function of the k_2^H/K_1^0 ratio at acid pHs. If such a ratio tends to zero, each molecule will only exchange n_1 electrons; if it tends to infinity, each molecule will exchange $(n_1 + n_2)$ electrons. By no means can the proposed mechanism lead to maxima in the plot of I vs pH, unlike in the previous case.

The influence of catalysis on the mechanism in Scheme 2 is evident in the behaviour of *o*- and *p*-nitrophenol derivatives[11,12]. The competitive reactions in the ECE mechanism of these compounds arise from a dehydration reaction subject to basic catalysis, in which case $k_2 = k_2^0 + k_2^{OH}[OH^-]$, and from the quasi-equilibrium dissociation of an H^+ ion ($K_1 = K_1^0/[H^+]$). At a sufficiently high pH, the height

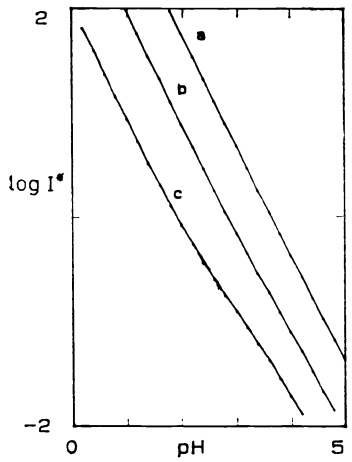

FIG. 3

Plot of $\log [(i_M - i_L)/(i_L - i_D^1)] = \log I^*$ vs pH for the example of Fig. 2

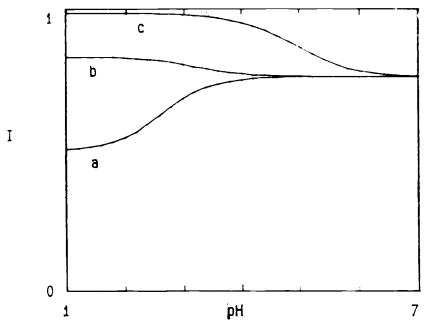

FIG. 4

Plot of I vs pH from Eq. (*32*). All parameters are the same as in Fig. 2, with the exception of $K_1^0 = 10^3$ and k_2, which was assumed to be $k_2 = k_2^0 + k_2^H[H^+]$, with $k_2^0 = 0{\cdot}5$ and $k_2^H = 0$ (curve a), $1 . 10^3$ (curve b) and $1 . . 10^5$ s^{-1} (curve c)

of the wave is a function of the $k_2^{OH}K_w/K_1^0$ ratio, similarly to the previous case. For *p*-nitrophenol, such a ratio tends to zero, so it yields a wave corresponding to the exchange of n_1 electrons[12]; for *o*-nitrophenol, the aforesaid ratio is rather large, so it yields a wave corresponding to the exchange of $(n_1 + n_2)$ electrons[11].

The authors wish to express their gratitude to the Dirección General de Investigación Científica y Técnica (DGICyT) *for financial support granted through Project* PB 88-0283.

REFERENCES

1. Saveant J. M.: Bull. Chim. Soc. Fr. *1967*, 493.
2. Rusling J. F., Segretario J. P., Zuman P.: J. Electroanal. Chem. Interfacial Electrochem. *143*, 291 (1983).
3. Moreno L., Blázquez M., Domínguez M., Roldán E.: J. Electroanal. Chem. Interfacial Electrochem. *185*, 119 (1985).
4. Rodríguez-Mellado J. M., Ruiz J. J.: J. Electroanal. Chem. Interfacial Electrochem. *119*, 177 (1986).
5. Segretario J. P., Zuman P.: J. Electroanal. Chem. Interfacial Electrochem. *214*, 237 (1986).
6. Segretario J. P., Slesznski N., Zuman P.: J. Electroanal. Chem. Interfacial Electrochem. *214*, 259 (1986).
7. Blázquez M., Jiménez M., Camacho L., Domínguez M.: J. Electroanal. Chem. Interfacial Electrochem. *243*, 309 (1988).
8. Lund H.: Acta Chem. Scand. *17*, 2325 (1963).
9. Marín Galvín R., Rodríguez-Mellado J. M.: J. Electroanal. Chem. Interfacial Electrochem. *250*, 399 (1988).
10. Muñoz E., Avila J. L., Camacho L.: J. Electroanal. Chem. Interfacial Electrochem. *284*, 445 (1990).
11. Heras A. M., Muñoz E., Avila J. L., Camacho L., Cruz J. L.: J. Electroanal. Chem. Interfacial Electrochem. *243*, 293 (1988).
12. Heras A. M., Muñoz E., Avila J. L., Camacho L.: Electrochim. Acta *32*, 1495 (1987).
13. Volke J.: Collect. Czech. Chem. Commun. *23*, 1486 (1958).
14. Laviron E.: Bull. Chim. Soc. Fr. *1961*, 2325.
15. Nakaya J.: Nippon Kagaku Zasshi *81*, 1731 (1960); Chem. Abstr. *56*, 2275 (1962).
16. Koutecký J.: Collect. Czech. Chem. Commun. *20*, 116 (1955) and *21*, 1056 (1956).
17. Smith D. E., McCord T. G., Hung H. L.: Anal. Chem. *39*, 1147 (1967).